CUBESPEC OPTICAL PAYLOAD

Gert Raskin[(1)], Jeroen De Maeyer[(2)], Sibo Van Gool[(1)], Leonardo Peri[(2)], Jorden Windey[(1)], Pierre Royer[(1)], Wim De Munter[(2)], Wannes Verstraeten[(1)], Jakob Pember[(1,3)], Tjorven Delabie[(4)], Maddalena Reggiani[(1)], Philippe Neuville[(1)], Dominic Bowman[(5,1)], Hugues Sana[(1)], Andrew Tkachenko[(1)], Dirk Vandepitte[(2)], Bart Vandenbussche[(1)]

[(1)]*Institute of Astronomy, KU Leuven, Celestijnenlaan 200D, 3001 Leuven, Belgium*
[(2)]*Department of Mechanical engineering, KU Leuven, Celestijnenlaan 300, 3001 Leuven, Belgium*
[(3)]*School of Mathematical and Physical Sciences, Macquarie University, NSW 2109, Australia*
[(4)]*arcsec, Blijde Inkomststraat 22, 3000 Leuven, Belgium*
[(5)]*School of Mathematics, Statistics and Physics, Newcastle University, Newcastle upon Tyne NE1 7RU, UK*

ABSTRACT

CubeSpec is an ESA in-orbit-demonstration mission, based on a 12-unit CubeSat, that targets high-resolution astronomical spectroscopy. It is developed and funded in Belgium and scheduled for launch early 2026. The main parts of CubeSpec's optical payload are an off-axis Cassegrain telescope, a high-resolution spectrograph, and a fine-guidance system. The primary mirror of the telescope has a rectangular shape, matched to the CubeSat form factor to maximise the aperture, covering approximately the surface area of two CubeSat units. The prism cross-dispersed echelle spectrograph delivers a spectral resolution of $R = 55\,000$ and covers the wavelength range from 420 to 620 nm in a single exposure. A fine steering mirror and a fine-guidance sensor provide accurate centring of the source image on the spectrograph slit to compensate for spacecraft pointing errors and jitter. Fitting these sub-systems inside the available payload volume (slightly more than 6U or half the spacecraft volume) made their optical design a technological challenge. To accommodate the large temperature excursions endured by the spacecraft during each orbit, the opto-mechanical design of both the telescope and the spectrograph is highly athermalised. In this contribution, we present the complete optical design as well as crucial aspects of the opto-mechanical design of the CubeSpec payload.

1 INTRODUCTION

The goal of the CubeSpec mission is to demonstrate the feasibility of astronomical spectroscopy from a 12-unit CubeSat. The prime science case for this ESA in-orbit demonstration mission is to unravel the interior of massive stars through asteroseismology using high-cadence monitoring of the variations in the spectral line profiles over the course of several months [1]. This requires a high-resolution spectrograph ($R = \lambda/\Delta\lambda \geq 50\,000$) and a telescope with a sufficiently large aperture to obtain spectra with a large signal-to-noise ratio (SNR ≥ 200). CubeSpec is designed and built at KU Leuven University (Belgium) with the ambition to provide the broader astronomical community with a generic solution for affordable space-based spectroscopy. With only minimal hardware changes, it is possible to tune the design of the spectrograph to a wide variety of science cases as long as the targets are sufficiently bright.

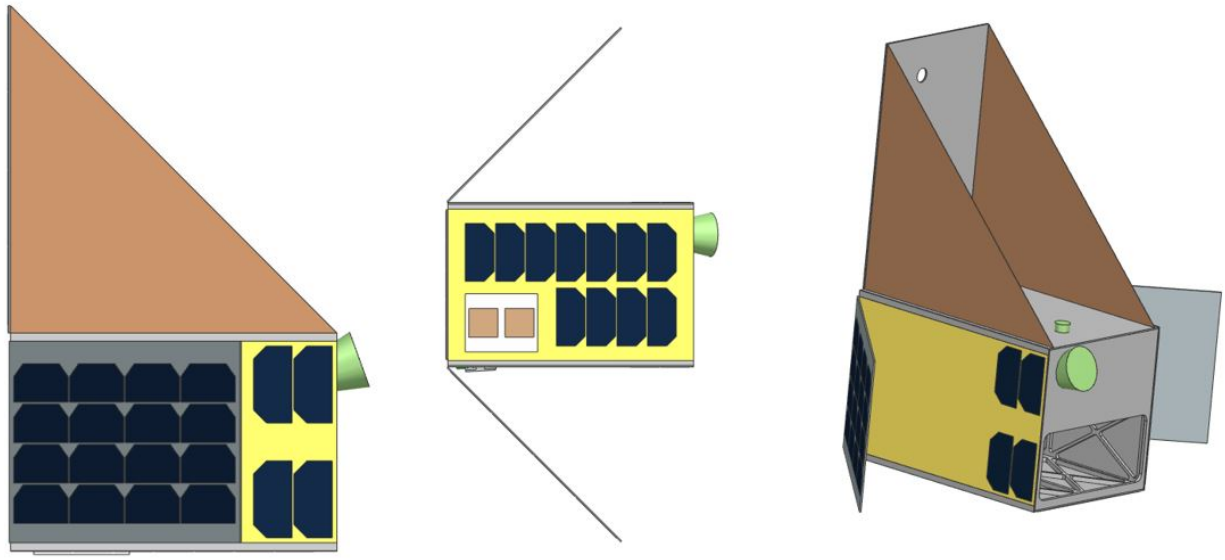

Figure 1: Preliminary design of the 12U CubeSpec spacecraft. The telescope is located behind the rectangular aperture at the bottom right The green cones represent the field of view of the star trackers.

Although the performance of attitude determination and control systems (ADCS) for CubeSats substantially increased in recent years [2], it still is insufficient to bring the spacecraft pointing accuracy and stability to the arcsec-level of the width of the entrance slit of the spectrograph. Therefore, we equipped the instrument with a fine steering mirror (FSM) that operates in closed loop with a fine-guidance sensor (FGS), complementing the ADCS in its task to stabilise the star image at the focus of the telescope on the spectrograph slit.

The original CubeSpec concept was based on a 6U CubeSat with a 4U payload and only two units for the spacecraft bus [3]. However, after several design iterations it turned out that the volume allocation of the latter was insufficient. Reducing the payload space envelope was not possible without compromising the science requirements of the mission. Therefore, we decided to increase the CubeSpec volume to a 12U CubeSat. In turn, the payload is now allowed to occupy a little more than six units, relaxing some of the tight optical and opto-mechanical design constraints. At the same time, we were able to slightly increase the telescope aperture and implement more efficient stray light baffles in the spectrograph.

A complete overview of the CubeSpec mission is presented in [4]. In Figure 1 we show the preliminary layout of the 12U CubeSat. An overview of the CubeSpec optical payload is shown in Figure 2. To make optimal use of the available space, the spectrograph is mounted on a bench parallel and below the primary mirror of the telescope. Apart of pointing correction, the FSM also takes care of folding the telescope beam into the spectrograph.

2 CASSEGRAIN TELESCOPE

2.1 Optical design

Designing a telescope for a CubeSat is a challenging endeavour, especially in case it is used for high-resolution spectroscopy. As the light from the observed targets will be strongly dispersed and spread out over a very large quantity of pixels on the image sensor, the quantity of collected photons and hence the size of the telescope aperture must increase accordingly. Obviously, this conflicts with the

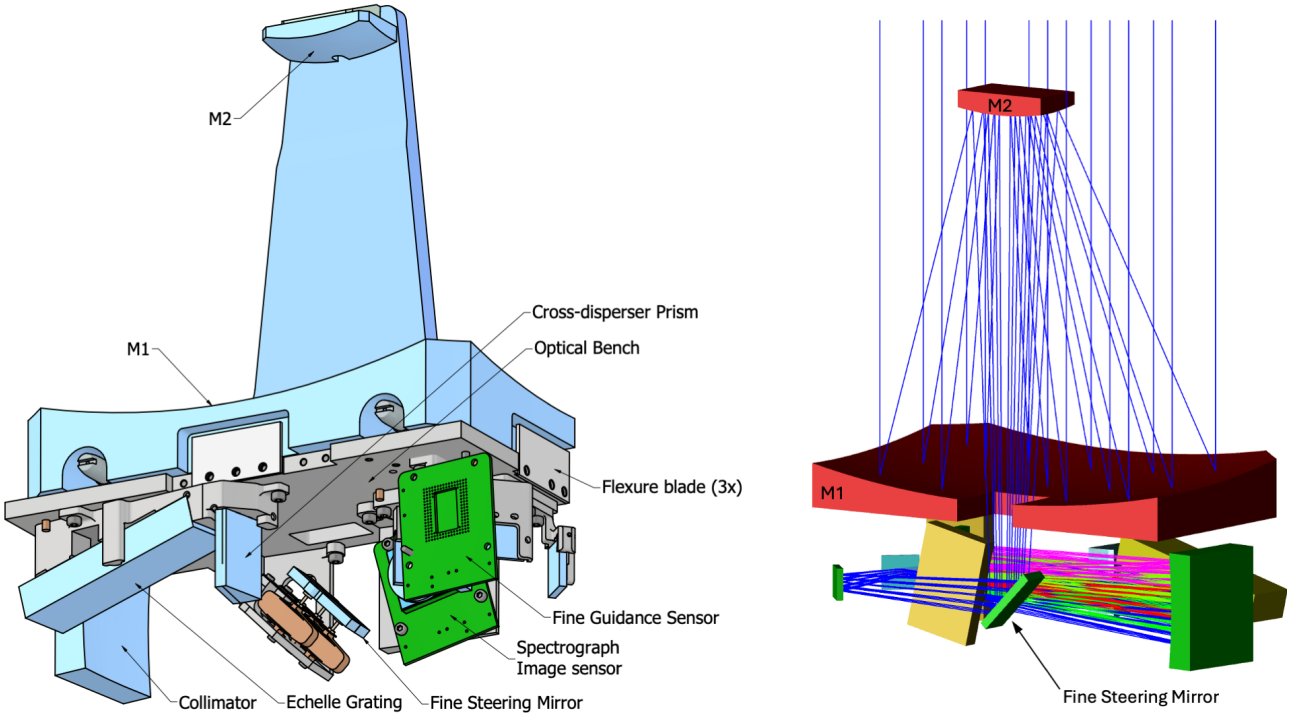

Figure 2: Overview of CubeSpec opto-mechanical layout (left) and optical raytrace, shown from the other side (right).

limited space envelope inside a CubeSat. Maximising the aperture almost automatically leads us to a rectangular shape and this excludes a lens-based design. A reflective telescope on the other hand can be readily designed from rectangular mirrors and this is what we have done for CubeSpec, with a primary mirror that roughly fills the surface area of two CubeSat units.

The CubeSpec telescope does not need to cover a wide field of view. It will only observe individual point sources and hence the "science field" of the telescope can be very small, only covering the entrance slit of the spectrograph that measures little more than a few arcsec. To allow the reliable acquisition of the star image on the slit, a total field of view of ±10 arcmin is largely sufficient. Excellent image quality is only required in the central part of the field where the slit is located. This can be easily achieved by a classical Cassegrain telescope consisting of a parabolic primary (M1) and hyperbolic secondary (M2) mirror. To have the telescope light beam entering the spectrograph at a convenient location and to simplify the mounting of M2 on a single structural beam, the telescope has an off-axis layout with the optical axis close to the edge of M1 (see Figure 2). The focal length of the telescope is 1600 mm and the entrance aperture measures 184 x 96 mm^2 (f/8.7 – f/16.7). Because of the very small field of view and the strong curvature of M1, the obscuration by M2 is very small ($< 10\%$ in surface area).

2.2 Opto-mechanical design

Although we have increased the CubeSat volume from 6U to 12U, the payload space envelope in still tight. This forces us to keep the axial separation between M1 and M2 small ($\approx$ 180 mm). As a consequence, the curvature of M1 has to be quite strong. The manufacturing of a very fast parabolic mirror ($\approx f/1$) is complicated but feasible. However, the strong curvature also poses challenging constraints on the alignment of M2 with respect to M1, as well as on the thermal stability of this alignment. To avoid unacceptable image quality degradation in the telescope focal plane, the axial

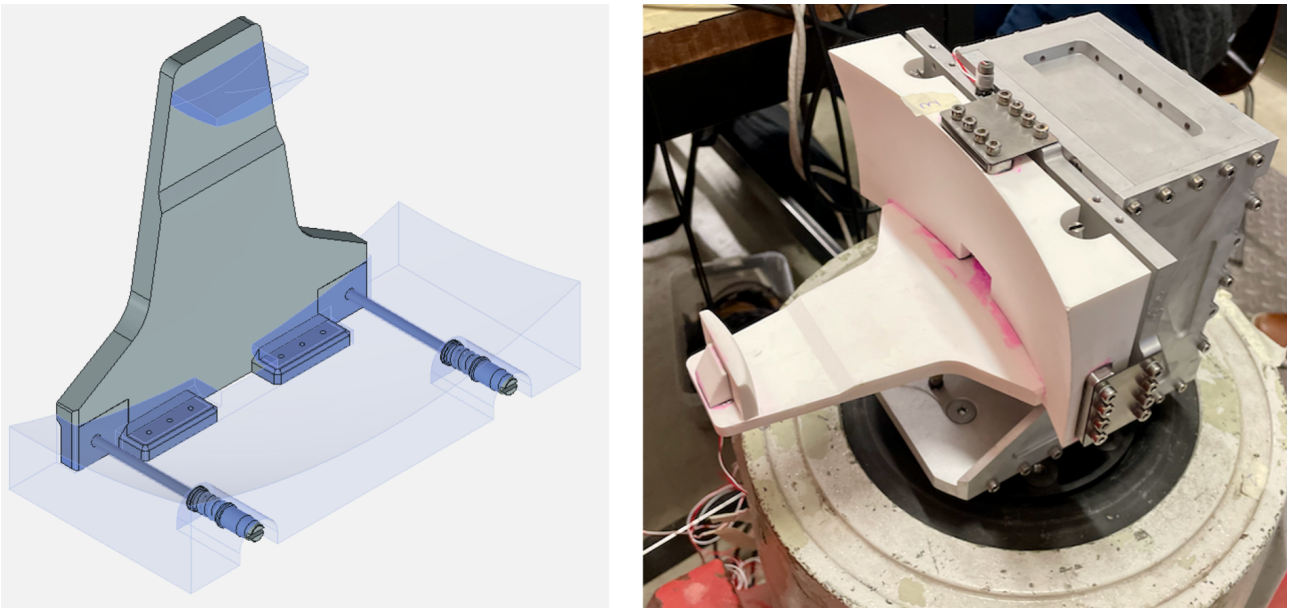

Figure 3: Glass-ceramic telescope design with transparent mirrors (left) and Macor qualification model mounted on a shaker for vibration tests (right).

position of M2 must be aligned and maintained with an accuracy of not more than a few μm. The lateral misalignment of M2 can be slightly larger. Especially the stability of the M2 position during the wide temperature excursions that the payload experiences during each orbit (> 30 K) is problematic. Even with a beam made of Invar (CTE $\approx 10^{-6}$ K^{-1}) between both mirrors, the thermal expansion of the M1-M2 structure ($> 5\,\mu$m) exceeds the alignment error budget. A straightforward solution, although mechanically complicated to implement, is to produce both the telescope mirrors as well as the separating beam from the same low-expansion glass-ceramic material. This results in an extremely stable quasi-monolithic telescope. We selected Cordierite (Kyocera) as ceramic material because it has a sufficiently low CTE (< 0.2 x 10^{-6} K^{-1}) to make make the thermal expansion of the M1-M2 structure negligible, and its stiffness is about 50% higher compared to Zerodur or ULE.

While the Cordierite beam offers a near-perfect solution from the thermal point of view, it is mechanically more fragile and more sensitive to shock and vibration loads than a metal beam. To ensure a reliable attachment of the beam on M1, we designed a connection that consists of a combination of adhesive bonding (3M Scotch-Weld 2216B/A epoxy) and two spring-loaded bolts. M2 is bonded to the beam by glue only. As a starting point for the mechanical qualification of a monolithic Cordierite telescope, we constructed a model made of Macor (Corning), a conventionally machinable ceramic material with slightly reduced mechanical performance compared to Cordierite. Figure 3 shows a 3D view of the design of the Cordierite telescope as well as the Macor test telescope mounted on shaker during a qualification campaign. It was exposed to and survived sine and random vibrations in different orientations as can be expected during typical launch conditions.

The telescope is attached to the optical bench via three flexure blades that are glued on the primary mirror.

3 HIGH PRECISION POINTING

Because the pointing performance of the spacecraft's ADCS is not good enough to stabilise the star image with arcsec-level precision on the entrance slit of the spectrograph, we added a high-precision pointing platform (HPPP) to the CubeSpec payload [5]. This HPPP consists of a fine steering mirror

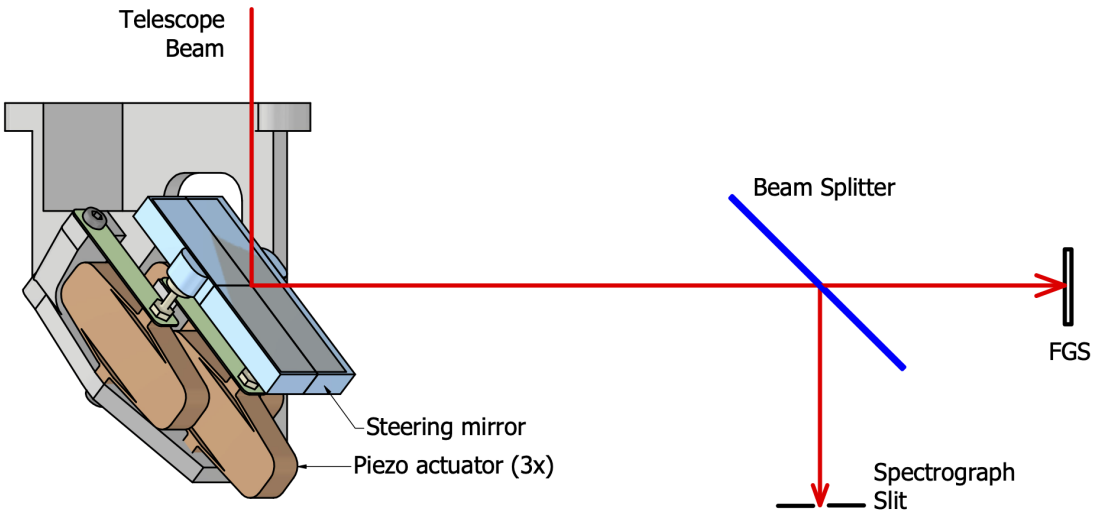

Figure 4: Tip/tilt fine steering mirror at the left as part of the HPPP.

(FSM) and a fine guidance sensor (FGS). The FSM consists of a 45° folding mirror, attached via three flexure rods to three amplified piezoelectric actuators to provide tip/tilt action (Figure 4). This mirror folds the telescope beam behind M1 and projects it on the spectrograph slit. We use the FSM to correct pointing errors and spacecraft jitter, and to actively stabilise the star image inside the slit. The large back focal length of the telescope provides the FSM with a 170-mm optical lever. This results in an angular stroke of $\pm 0.4°$, corresponding to ± 1.25 arcmin (horizontal plane) or ± 2.5 arcmin (vertical plane) on the sky. The first eigenmode of the FSM is located around 800 Hz, complying with launcher requirements and guaranteeing sufficient margin for the HPPP control loop without exciting any structural mode.

A dichroic beam splitter reflects the incident beam to the entrance slit of the spectrograph. The wavelengths outside the spectral range of interest for the spectrograph ($\lambda < 420$ nm and $\lambda > 620$ nm) are transmitted to the FGS which is conjugated with the slit plane. The position of the star image on the FGS serves as the reference signal for the feedback loop of the fine steering mirror. The FGS is a CMOS image sensor of the same type as the spectrograph detector (Section 4.2). It can be read out at speeds up to 40 Hz. The HPPP control loop runs at the same frequency.

4 SPECTROGRAPH

4.1 Dispersion

Arguably the best solution for a high-resolution spectrograph that has to sample a very broad wavelength range in a single exposure, is a cross-dispersed echelle spectrograph. An echelle is a diffraction grating with a coarse groove density and a groove shape optimised for operating at large angles of incidence (i.e. with a large blaze angle θ_B) and in high diffraction orders. Higher diffraction orders lead to stronger dispersion of the incident light and hence higher spectral resolution, but also imply shorter free spectral range and overlapping diffraction orders. With a low-dispersion cross disperser, operating perpendicularly to the echelle dispersion, we can separate the overlapping diffraction orders and obtain an almost rectangular wide-range high-resolution spectrum that is well matched to standard two-dimensional image sensors.

As main disperser for the CubeSpec spectrograph, we selected a steep echelle grating ($\theta_B = 76°$) to maximise spectral resolution that has a groove spacing of 41.6 gr/mm (Newport – Richardson Grating

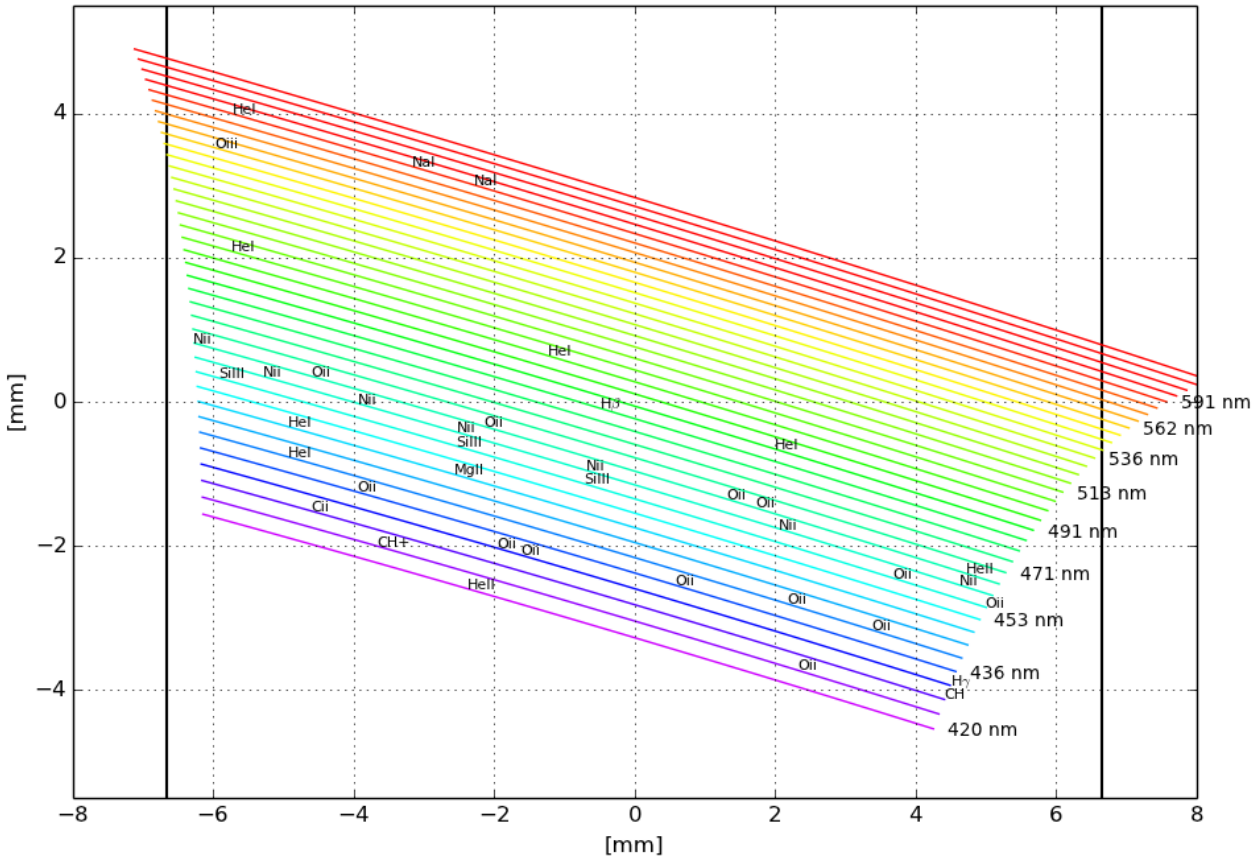

Figure 5: Layout of the echelle spectrum on the image sensor, with labels for the most relevant stellar lines of interest (the thick vertical lines correspond with the edges of the sensor).

Lab). The groove spacing defines the length of the diffraction orders and allows us to match the spectral format to the length of the image sensor. Cross dispersion is provided by a prism used in double pass. The prism is made from high-dispersion N-SF6HT (Schott), a flint glass with fairly good transmission down to the bluest wavelengths (420 nm). While standard SF6 has even higher blue transmission, it could be prone to radiation darkening. N-SF6HT has been radiation tested by ESA [6], showing that after a conservative exposure dose of 11 krad, the internal transmission of the glass drops from 92% to a still acceptable level of 78% at 420 nm (10 mm glass thickness). The combination of this echelle grating and prism results in a spectral resolution of 55 000 (requirement: $R \geq 50\,000$) and a wavelength coverage from 420 to 620 nm. Figure 5 shows a simulation of the 2-dimensional echelle spectrum on the image sensor. The reddest orders are slightly truncated but no important spectral information is lost.

4.2 Optical layout

The CubeSpec spectrograph optics (Figure 6) are designed around a Schmidt camera used in double pass. A Schmidt camera is a catadioptric system consisting of a spherical mirror and an aspherical corrector lens (Schmidt corrector plate) located at the centre of curvature of the mirror. It provides excellent image quality over a large field of view. The original CubeSpec design used a three-mirror anastigmat (TMA) instead of a Schmidt camera [7]. However, the TMA solution proved to be much more critical to align and much more expensive to manufacture. Because a spherical mirror has no preferred axis, it is much less sensitive to alignment errors. The Schmidt system serves as collimator for the telescope beam and as camera to focus the dispersed spectrum on the detector. Like the

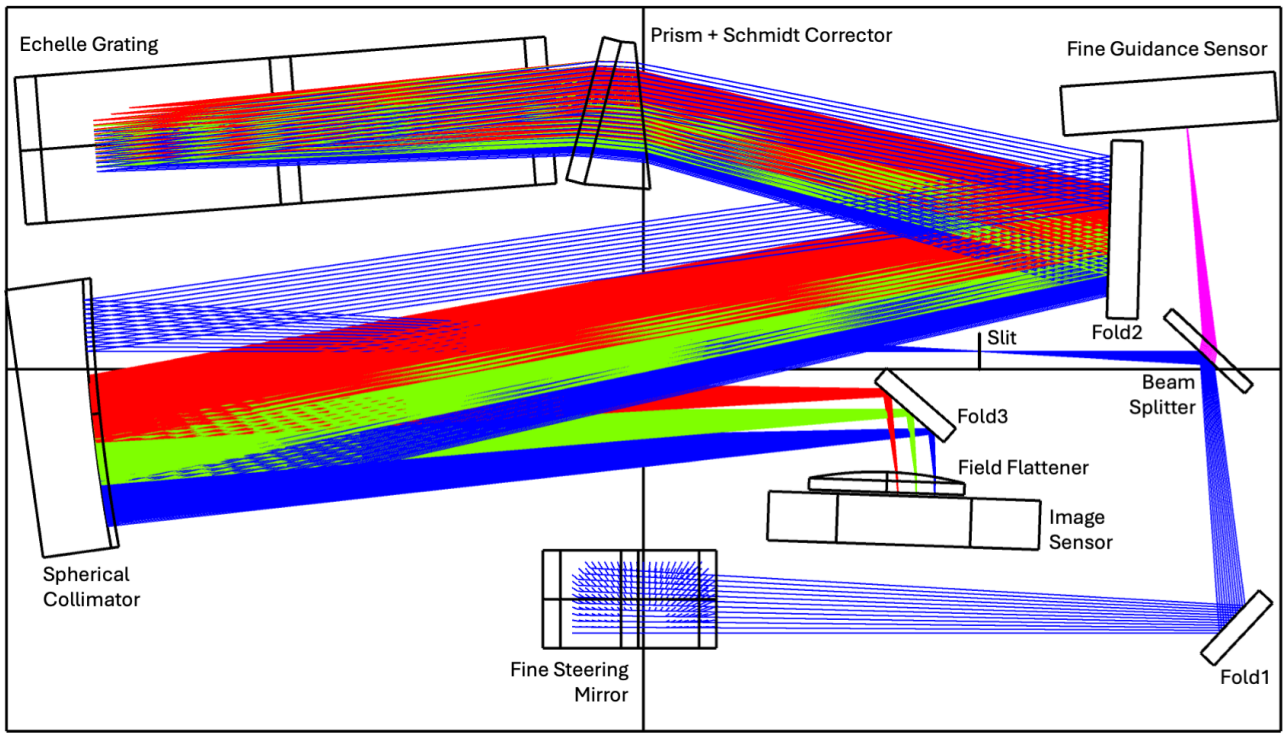

Figure 6: Spectrograph raytrace. The telescope beam enters the spectrograph perpendicularly to the plane of the figure through a rectangular hole in the primary mirror and in the optical bench, behind the Fine Steering Mirror.

telescope, this Schmidt camera is an off-axis system that completely avoids light loss due to central obscuration.

To limit the number of optical surfaces and to save space on the optical bench, the corrector plate is cemented on the exit surface of the prism. Consequently, it is slightly tilted with respect to the incident and dispersed light beams. Moreover, because of space limitations the corrector plate is located slightly in front of the centre of curvature of the spherical mirror ($\Delta \cong 30$ mm). However, both these deviations from the ideal configuration have a negligible impact on the image quality. The corrector is an off-axis section of a 4^{th}-degree even aspherical surface.

A disadvantage of the Schmidt-camera solution is that it produces a curved image plane. Hence, we need a field flattener lens to image the curved spectrum on a flat image sensor. This field flattener is a plano-convex fused silica lens that is directly glued on the image sensor, in replacement of its cover glass. Additionally, it provides the image sensor with some radiation protection. This sensor is a 2k x 2k 6.5-μm pixels thinned back-illuminated CMOS image sensor from Gpixel (GSENSE202BSI). Apart from the flexible and fast read-out of the CMOS circuit, this sensor offers excellent quantum efficiency (90% at 500 – 600 nm) and low read noise ($< 2\,e^-$). Sensor read-out and control electronics are designed in-house at KU Leuven around a Zynq-7000 (Xilinx) FPGA system.

To fit the spectrograph in the available volume behind the primary mirror of the telescope, we added three flat mirrors to the optical system that fold the incident and dispersed beams, minimising its total footprint. Because of the large number of mirror reflections, high-quality mirror coatings are of prime importance for the overall throughput. All the spectrograph mirrors will be coated with a dielectric mirror coating that has a reflectivity above 99% over the 420 – 620 nm wavelength range.

The spectrograph optics are mounted on an optical bench, located just below and with approximately the same dimensions as the primary mirror of the telescope. The material for the bench is Invar to ensure thermal stability for the spectrograph.

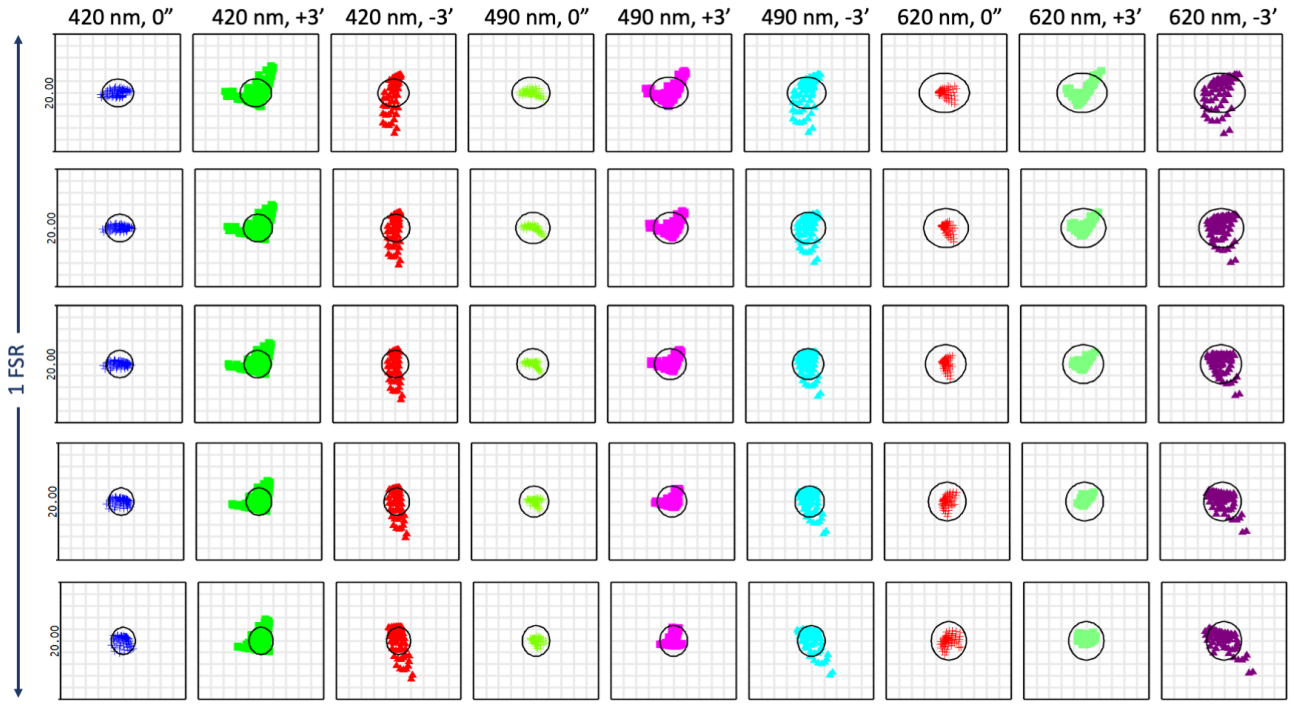

Figure 7: Spot diagrams along the free spectral range (FSR) of 3 spectral orders (420, 490 and 620 nm), with the fine steering mirror in neutral position and correcting for pointing errors of ±3 arcmin. The spot box size is 20 x 20 μm (for reference, the spectrograph slit dimensions are 20 x 50 μm).

4.3 Spectrograph slit

Although the image quality of the CubeSpec telescope is diffraction limited in the central part of the field of view, a rectangular slit is added at the entrance of the spectrograph. The width of this slit, and not the size of the telescope's Airy disk, will define the spectral resolution. The advantage of the slit is that the fidelity of the spectra will no longer be affected by spacecraft jitter and that the requirements on pointing stability can be substantially reduced. Pointing errors larger than the angular extent of the slit will now only result in a loss of throughput (i.e. when the star image does not fall inside the slit), without affecting the spectral quality of the acquired data. The dimensions of the slit are 2.6 x 6.5 arcsec (20 x 50 μm), with the smallest dimension corresponding to the main dispersion direction. In cross-dispersion direction, 2.5x larger pointing errors are accepted as this does not affect the spectral resolution.

5 PAYLOAD PERFORMANCE

CubeSpec's optical system, consisting of both the telescope and the spectrograph, offers excellent image quality, as illustrated by the spot diagrams in Figure 7. All spots are substantially smaller than the slit width. This means that the spectral resolution is entirely defined by the width of the slit in main dispersion direction (i.e. vertical in the figure) and that it is not affected by any aberrations produced by the spectrograph optics. The fine steering mirror can be used to homogenise the illumination of the slit by dithering the image around inside the slit. The image movement by the fine steering mirror also leads to a small shift of the pupil in the spectrograph. A correction of 3 arcmin moves the footprint of the beam on the echelle grating by 2.7 mm (ca. 4% pupil shift). This has a minor effect on the image quality and is completely negligible for the spectral resolution.

Figure 8 shows the predicted signal-to-noise ratio (SNR) as a function of stellar magnitude (m_V) for

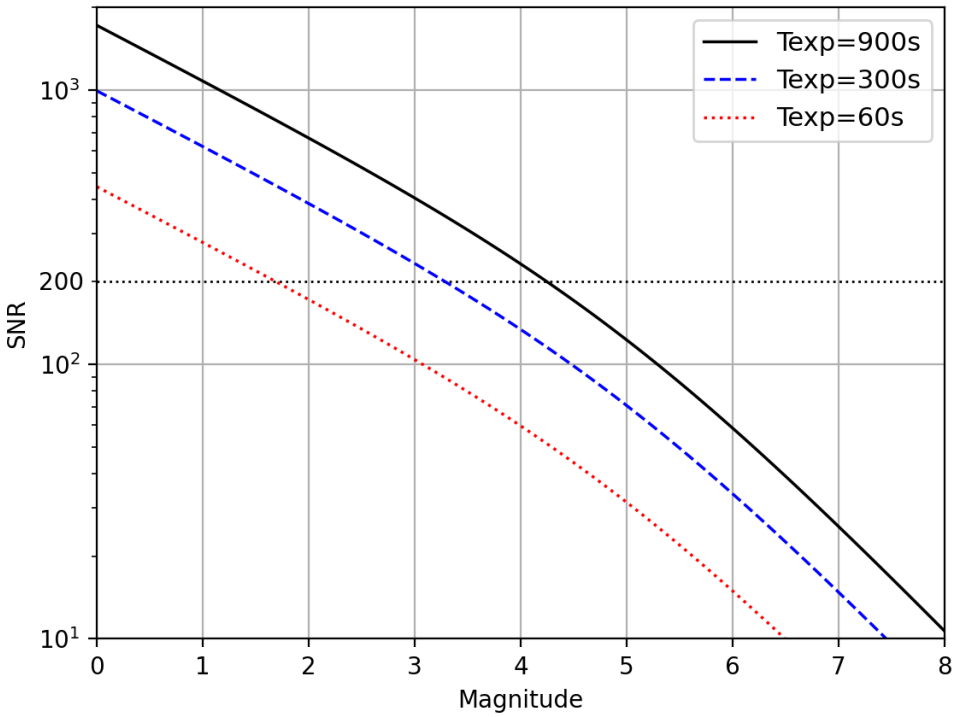

Figure 8: Estimated SNR in function of stellar magnitude for various exposure times at $\lambda = 500$ nm and R = 55 000. The dashed horizontal line at SNR = 200 corresponds with the requirement of the main science case for CubeSpec.

exposure times of 1, 5, and 15 minutes at $\lambda = 500$ nm and $R = 55\,000$. For this calculation, we used conservative estimates for the throughput of all optical components, and the quantum efficiency and noise properties of the image sensor. Additionally, we account for a slit loss of 40% due to pointing jitter, meaning the star image could fall (partially) outside the slit during the observation. The main science case of CubeSpec requires an SNR $\simeq 200$. This is obtained with an exposure time of less than 15 minutes on a 4^{th} magnitude star. All the stars in the CubeSpec target list are brighter than $m_V = 4$ [1].

6 PAYLOAD VARIANTS

While the first CubeSpec version, presented in this contribution, focuses on high-resolution spectroscopy for carrying out asteroseismology on massive stars, the payload optics are designed to be very generic. With only minimal modifications to the optical system, the instrument design can be customised to different spectral resolutions (from *R* less than 100 up to 70 000) and wavelength ranges (between 250 nm and 950 nm). The hardware changes involved would typically consist of swapping the echelle grating and the cross-disperser prism for a different type of disperser (e.g. a double-pass Amici prism for very low spectral resolutions), and optimising the mirror and beam-splitter coatings for the specific wavelength range of interest. This allows us to adapt the optical design conveniently to a wide variety of science cases as long as the brightness of the targets can be matched to the limited telescope aperture. This way, CubeSpec opens up a promising path to affordable space-based astronomical spectroscopy.

ACKNOWLEDGEMENTS

For the development of the HPPP, the authors gratefully acknowledge the financial support of FWO Vlaanderen through project S000719N.

REFERENCES

[1] D. M. Bowman, B. Vandenbussche, H. Sana, *et al.*, "The CubeSpec space mission. I. Asteroseismology of massive stars from time series optical spectroscopy: science requirements and target list prioritisation," *Astronomy & Astrophysics*, vol. 658, 2022. DOI: 10.48550/ARXIV.1805.11848.

[2] M. Knapp and S. Seager, "ASTERIA: A CubeSat Enabling High Precision Photometry in a Small Package," in *42nd COSPAR Scientific Assembly*, vol. 42, Jul. 2018, E4.1-4-18, E4.1-4–18.

[3] B. Vandenbussche, G. Raskin, P. Royer, *et al.*, "CubeSpec - Enabling spectroscopy from a CubeSat platform.," in *Proc. of the Small Satellites, System and Services Symposium (4S)*, Vilamoura, Portugal, 2022.

[4] J. De Maeyer, B. Vandenbussche, G. Raskin, *et al.*, "CubeSpec: High resolution spectroscopy from a CubeSat platform," in *Proc. of the Small Satellites, System and Services Symposium (4S)*, Palma de Mallorca, Spain, 2024.

[5] W. D. Munter, J. D. Maeyer, L. Peri, and D. Vandepitte, "High Precision Pointing Platform Performance Simulations For Small Spacecraft Missions," in *Proc. Guidance, Navigation and Control Conference (GNC)*, Sopot, Poland, 2023. DOI: [10.5270/esa-gnc-icatt-2023-111].

[6] E. B. Cugny, N. Karafolas, and Z. Sodnik, "The ESA radglass activity: A radiation study of non rad-hard glasses," en, *International Conference on Space Optics*, p. 9, 2016.

[7] G. Raskin, T. Delabie, W. D. Munter, *et al.*, "CUBESPEC: Low-cost space-based astronomical spectroscopy," in *Proc. SPIE 10698, Space Telescopes and Instrumentation 2018: Optical, Infrared, and Millimeter Wave*, Austin, Texas (US), 2018. DOI: 10.1117/12.2314074.